DALTON

Pentanuclear copper(II) complexes with the novel 6-(phenylethynyl)-2-pyridonate ligand: synthesis, structures and magnetic properties

Allan A. Doyle, Simon Parsons, Gregory A. Solan and Richard E. P. Winpenny*

Department of Chemistry, The University of Edinburgh, West Mains Road, Edinburgh, UK EH9 3JJ

Three pentanuclear copper(II) complexes, $[Cu_5(OMe)_2(CF_3CO_2)(pehp)_6(Cl)]$ **1**, $[Cu_5(OMe)_2(CF_3CO_2)(pehp)_6(NO_3)]$ **2** and $[Cu_5(OH)(CF_3CO_2)_3(pehp)_6]$ **3**, have been prepared *via* the solid-state reaction of hydrated copper(II) nitrate with the sodium salt of the novel ligand, 6-(phenylethynyl)-2-pyridone (Hpehp) in the presence of sodium trifluoroacetate. Crystal structural analysis at 220 K of **1**–**3** reveals capped-butterfly arrangements of the five copper atoms with the two shortest Cu · · · Cu vectors in **1** and **2** [3.024(6)–3.050(3) Å] occurring between the caps and the wingtips while in **3** the wingtip–cap distances are more asymmetric with one short [3.042(7) Å] and one long [3.638(7) Å] Cu · · · Cu vector. Mass spectroscopic studies of **1**–**3** show fragmentation patterns consistent with the observed structures, while magnetic studies of the complexes indicate antiferromagnetic exchange coupling within the Cu_5 cores and $S = \frac{1}{2}$ ground states for all compounds. The trifluoroacetate adduct of Hpehp, Hpehp·$0.5CF_3CO_2H$ was synthesised in three steps from 2-bromo-6-benzyloxypyridine *via* 2-benzyloxy-6-(phenylethynyl)pyridine and the single crystal X-ray structure of Hpehp was also determined.

The controlled synthesis of polymetallic complexes with specific magnetic properties continues to provide a motivation for research. The nature of the ligand is crucial in governing the nuclearity and arrangement of the resulting species,[1–4] while substituents on a given ligand may play a more subtle but as significant a role in the way the cluster assembles.[5–9]

The 2-pyridonate family of ligands has been widely employed in recent years in co-ordination chemistry due in part to the variety of bonding modes possible.[5] In particular, a range of polynuclear complexes are accessible by shrewd choice of 6-substituted-2-pyridonate. For example, the solid-state reactions of copper(II) nitrate with either 6-chloro-2-pyridonate (chp), 6-fluoro-2-pyridonate (fhp) or 6-methyl-2-pyridonate (mhp) gave respectively homoleptic dinuclear,[6] tetranuclear[7] or hexanuclear[8] copper(II) species. In contrast, the combination of carboxylate and the 6-substituted-2-pyridonate [6-bromo-2-pyridonate (bhp), chp or mhp] ligands gave exclusively octanuclear copper(II) complexes.[9] To investigate the factors that contribute to the nature of the polynuclear assembly we have sought to extend the range of substituents located at the six position on the pyridonate ring. Here we report the synthesis of the protonated phenylethynyl derivative, 6-(phenylethynyl)-2-pyridone (Hpehp), and the reaction of the sodium salt of its anion with hydrated copper(II) nitrate.

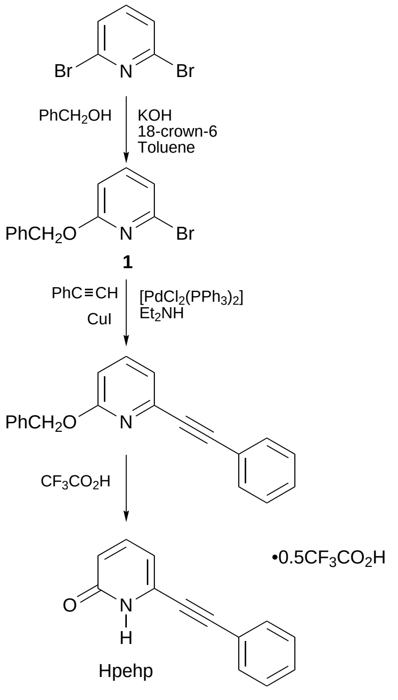

Scheme 1 Synthetic route for the formation of Hpehp·$0.5CF_3CO_2H$ from 2,6-dibromopyridine

Experimental

Hydrated copper(II) nitrate, 2,6-dibromopyridine, 1,4,7,10,13,16-hexaoxacyclooctadecane (18-crown-6), bis(triphenylphosphine)palladium dichloride, copper(I) iodide, phenylacetylene, diethylamine, trifluoroacetic acid and lanthanum nitrate hexahydrate were obtained from Aldrich. Solvents were used as obtained from suppliers.

Hydrogen and ^{13}C NMR spectra were recorded in $CDCl_3$ at room temperature on a Bruker AM-250 MHz spectrometer. Mass spectra were obtained by fast-atom bombardment (FAB) of samples in a 3-nitrobenzyl alcohol matrix on a Kratos MS50 spectrometer. Infrared spectra were recorded on a Perkin-Elmer Paragon 1000 FT-IR spectrometer as Nujol mulls (KBr or NaCl plates) or as KBr discs. The EPR measurements were made at Q-band (*ca.* 34.2 GHz) using a Bruker ESP300E spectrometer fitted with an ER4118CF cryostat. Analytical data were obtained on a Perkin-Elmer 2400 elemental analyser by the University of Edinburgh microanalytical service.

Preparation of compounds

6-(Phenylethynyl)-2-pyridone (Hpehp). The three-step synthesis of Hpehp from **1** was based on that reported for dipyridonylacetylene $[(C_5H_4NO)CC(ONC_5H_4)]$ (see Scheme 1).[10]

(*i*) 2-*Bromo*-6-*benzyloxypyridine.* A mixture of 2,6-dibromopyridine (5.03 g, 21.2 mmol), benzyl alcohol (2.64 g, 24.4 mmol), potassium hydroxide (2.60 g, 46.4 mmol) and 18-crown-6 (0.24 g, 0.91 mmol, 4 mol%) in toluene (70 cm^3) was heated under reflux, with a Dean–Stark apparatus, for 1 h.

After this time TLC [silica, cyclohexane–ethyl acetate (2 : 1)] indicated complete consumption of starting material. The reaction mixture was cooled and quenched by the addition of ice/water (50 cm^3). The layers were separated and the aqueous layer extracted into toluene (2 × 50 cm^3). The combined organic layers were dried over Na_2SO_4, filtered and evaporated to dryness to give 2-bromo-6-benzyloxypyridine as an orange liquid (5.59 g, 99.9%). IR (KBr, thin film, cm^{-1}) 1587, 1554, 1496 and 1437. NMR: ^1H, δ 7.54–7.25 (m, 6 H), 7.08 (dd, J_{HH} 7.5, J_{HH} 0.6, 1 H), 6.75 (dd, J_{HH} 8.2, J_{HH} 0.6 Hz, 1 H), 5.37 (s, 2 H, $PhCH_2$); $^{13}C-\{^1H\}$, δ 162.9 (s, C), 140.4 (s, CH), 138.3 (s, C), 136.4 (s, C), 128.3 (s, 2CH, Ph), 128.2 (s, 2CH, Ph), 127.9 (s, CH, Ph), 120.3 (s, CH), 109.6 (s, CH) and 68.3 (s, $PhCH_2$).

(*ii*) 2-*Benzyloxy*-6-*phenylethynylpyridine*. Copper(I) iodide (0.22 g, 1.16 mmol, 3 mol%) was added to a mixture of 2-bromo-6-benzyloxypyridine (10.08 g, 38.18 mmol), $[PdCl_2(PPh_3)_2]$ (0.18 g, 1.15 mmol, 3 mol%) and phenylacetylene (4.29 g, 42.1 mmol, 1.1 equivalents) in diethylamine (120 cm^3) under argon. The reaction mixture was allowed to stir at room temperature for 20 h after which time TLC [silica, hexane–ether (95 : 5)] indicated the absence of any starting material. The solvent was removed under reduced pressure and water (400 cm^3) added to the residue. The mixture was extracted into toluene (3 × 400 cm^3) and the combined organic layers dried over $MgSO_4$, filtered and the solvent removed to afford a brown sticky solid. The crude product was subjected to flash chromatography [silica, hexane–ether (100 : 1–95 : 5)] to give 2-benzyloxy-6-phenylethynylpyridine as a pale yellow solid. The solid was recrystallised from hexane to give pale yellow crystals (7.69 g, 70%). IR (KBr, cm^{-1}) 2208 [ν(C≡C)], 1582, 1489, 1440. M.p. 70.4–72.4 °C. NMR: ^1H, δ 7.63–7.48 (m, 5 H), 7.48–7.33 (m, 6 H), 7.17 (d, J_{HH} 7.1, 1 H), 6.78 [dd, J_{HH} 8.6, J_{HH} 0.8, Hz, 1 H], 5.44 (s, 2 H, $PhCH_2$); $^{13}C-\{^1H\}$ (62.9 MHz), δ 163.3 (s, C), 140.1 (s, C), 138.6 (s, CH), 136.9 (s, C), 131.9 (s, C), 128.7 (s, 2CH), 128.3 (s, CH), 128.2 (s, 2CH), 128.1 (s, 2CH), 127.8 (s, CH), 122.3 (s, C), 120.9 (s, CH), 111.2 (s, CH), 88.7 (s, *C*≡C), 88.5 (s, C≡*C*) and 67.8 (s, $PhCH_2$).

(*iii*) 6-(*Phenylethynyl*)-2-*pyridone* (*Hpehp*). A solution of 2-benzyloxy-6-phenylethynylpyridine (8.17 g, 28.7 mmol) in trifluoroacetic acid (120 cm^3) was stirred at room temperature for 4 d. The trifluoroacetic acid was stripped off under reduced pressure and the residue treated with benzene (50 cm^3) then re-evaporated. The residue was partitioned between 1 M sodium hydroxide solution (200 cm^3) and ethyl acetate (200 cm^3) and the layers separated. The aqueous layer was acidified to pH 1 by the addition of 6 M hydrochloride acid, then extracted into ethyl acetate (2 × 200 cm^3). The combined organic layers were dried over $MgSO_4$, filtered and the solvent removed to give a sticky brown solid. The crude product was then triturated with ether to give $Hpehp\cdot0.5CF_3CO_2H$ as an off-white solid (5.98 g, 83%). In general, $Hpehp\cdot0.5CF_3CO_2H$ was used in further reactions, but pure Hpehp could be obtained by recrystallisation from ethyl acetate (Found: C, 66.85; H, 3.75; N, 5.35. $C_{13}H_9NO\cdot0.5CF_3CO_2H$ requires C, 66.65; H, 3.75; N, 5.55%). IR (KBr disc, cm^{-1}) 2932 [ν(N−H)], 2213 [ν(C≡O)], 1687 [ν(C=O)], 1654, 1600. M.p. 173–175 °C. NMR: ^1H, δ 12.35 (s, 1 H, NH), 7.58–7.51 (m, 2 H), 7.41–7.20 (m, 4 H), 6.62 [dd, J_{HH} 9.2, J_{HH} 0.8, 1 H], 6.48 [dd, J_{HH} 6.8, J_{HH} 0.6 Hz, 1 H]; $^{13}C-\{^1H\}$ (62.9 MHz), δ 164.3 (s, C=O), 140.1 (s, CH), 131.9 (s, 2CH, Ph), 129.5 (s, CH, Ph), 129.3 (s, C), 128.3 (s, 2CH, Ph), 121.0 (s, C, Ph), 120.7 (s, CH), 111.7 (s, CH), 94.6 (s, *C*≡C) and 81.9 (s, C≡C).

$[Cu_5(OMe)_2(CF_3CO_2)(pehp)_6(Cl)]$ 1. Hydrated copper(II) nitrate (0.21 g, 0.87 mmol) and the sodium salt of $Hpehp\cdot0.5CF_3CO_2H$ (0.50 g, 1.75 mmol, prepared by deprotonation of the adduct with 1.5 equivalents of NaOH in MeOH, followed by evaporation to dryness) were mixed intimately together as solids. The dark green paste formed was extracted into CH_2Cl_2 (100 cm^3) and the resulting dark green solution was filtered. The filtrate was concentrated to 10 cm^3 and methanol (10 cm^3) was added to give green crystals of **1** (0.81 g, 55%) after 2–3 d (Found: C, 54.95: H, 3.35; N, 4.35. $C_{82}H_{54}ClCu_5F_3N_6O_{10}\cdot1.5CH_2Cl_2\cdot CH_3OH$ requires C, 54.80; H, 3.25; N, 4.55%). IR (KBr disc, cm^{-1}) 2216 [ν(C≡C)], 1676, 1589, 1560, 1492, 1261, 1203, 1027, 809, 754, 726 and 688. FAB-MS: significant peaks (*m*/*z*), possible assignments: 1625, $[Cu_5(OMe)(CF_3CO_2)(pehp)_6]$; 1513, $[Cu_5(OMe)(pehp)_6]$; 1450, $[Cu_4(OMe)(pehp)_6]$; 1256, $[Cu_4(OMe)(pehp)_5]$; 1224, $[Cu_4(pehp)_5]$; 1030, $[Cu_4(pehp)_4]$; 967, $[Cu_3(pehp)_4]$; 772, $[Cu_3(pehp)_3]$; 708, $[Cu_2(pehp)_3]$; 514, $[Cu_2(pehp)_2]$.

$[Cu_5(OMe)_2(CF_3CO_2)(pehp)_6(NO_3)]$ 2. Complex **2** was made using the procedure outlined for **1** but, after concentration of the filtrate, MeOH (10 cm^3) containing an excess of $La(NO_3)_3\cdot6H_2O$ was added to give green crystals of **2** (0.60 g, 40%) after 2–3 d (Found: C, 56.65; H, 2.95; N, 5.65. $C_{82}H_{54}Cu_5F_3N_7O_{13}\cdot1.5CH_3OH$ requires C, 56.70; H, 3.40; N, 5.55%). IR (KBr disc, cm^{-1}) 2213 [ν(C≡C)], 1671, 1589, 1546, 1289 [ν(O_2N−O)], 1202, 1022, 804, 760 and 717. FAB-MS: significant peaks (*m*/*z*) possible assignments: 1625, $[Cu_5(OMe)(CF_3CO_2)(pehp)_6]$; 1593, $[Cu_5(pehp)_6(CF_3CO_2)]$; 1512, $[Cu_5(OMe)(pehp)_6]$; 1480, $[Cu_5(pehp)_6]$; 1339, $[Cu_4(pehp)_5(CF_3CO_2)]$; 1256, $[Cu_4(OMe)(pehp)_5]$; 1224, $[Cu_4(pehp)_5]$; 1143, $[Cu_4(pehp)_4(CF_3CO_2)]$; 1030, $[Cu_4(pehp)_4]$; 967, $[Cu_3(pehp)_4]$; 772, $[Cu_3(pehp)_4]$; 708, $[Cu_2(pehp)_3]$.

$[Cu_5(OH)(CF_3CO_2)_3(pehp)_6]$ 3. The same procedure as used for **1** was followed, except that after concentration of the filtrate to 10 cm^3 it was allowed to stand at room temperature for 3 w to give green plates of **3** (0.16 g, 10%) (Found: C, 59.90; H, 3.75; N, 4.55. $C_{82}H_{49}Cu_5F_9N_6O_{13}\cdot2.4Hpehp$ requires C, 59.80; H, 3.05; N, 5.10%). IR (KBr, cm^{-1}) 3250 [ν(O−H)], 2217 [ν(C≡C)], 1666, 1603, 1534, 1492, 1358, 1294, 1261, 1205, 1158, 802, 757, 690 and 557. FAB-MS: significant peaks (*m*/*z*), possible assignments: 1513, $[Cu_5(CF_3CO_2)_2(pehp)_5]$; 1400, $[Cu_5(CF_3CO_2)(pehp)_5]$; 1287, $[Cu_5(pehp)_5]$; 1224, $[Cu_4(pehp)_5]$; 1030, $[Cu_4(pehp)_4]$; 967, $[Cu_3(pehp)_4]$; 772, $[Cu_3(pehp)_3]$; 708, $[Cu_2(pehp)_3]$; 515, $[Cu_2(pehp)_2]$.

Crystallography

Crystal data and data collection and refinement parameters for Hpehp and **1**–**3** are given in Table 1; selected bond distances and angles in Tables 2–4. The structure of **1** Hpehp was performed on the free ligand, and not on the trifluoroacetate adduct.

Data collection and processing. Data were collected using ω–θ scans on a Stoë Stadi-4 four-circle diffractometer equipped with an Oxford Cryosystems low-temperature device[11] operating at 220.0(2) K, using Cu-Kα radiation for Hpehp, **1** and **3** and graphite-monochromated Mo-Kα radiation for **2**. All data were corrected for Lorentz and polarisation effects. Data for **1**–**3** were corrected for absorption using ψ-scans. For **2** a lamina correction was used, based on 238 data, which gave T_{min} and T_{max} of 0.506 and 0.814 respectively. For **3** an ellipsoidal correction was used, based on 345 data, which gave T_{min} and T_{max} of 0.287 and 0.622 respectively.

Structure analysis and refinement. Following data reduction all structures were solved by direct methods (SIR 92[12] for Hpehp or SHELXS 86[13] for **1**–**3**) and refined by full-matrix least squares against *F* for Hpehp (CRYSTALS)[14] and F^2 for **1**–**3** (SHELXL).[15] In Hpehp and **3** all non-hydrogen atoms were refined anisotropically, whereas in **1** and **2** only the full-weight atoms constituting the complex were so refined, the solvent of crystallisation being modelled isotropically. Hydrogen atoms were placed in calculated positions in all structures. In **3** there is a two-fold rotational disorder in two of the three CF_3 groups;

Table 1 Experimental data for the X-ray diffraction studies of Hpehp and complexes **1**–**3**

Compound	Hpehp	**1**	**2**	**3**
Formula	$C_{13}H_9NO$	$C_{82}H_{54}ClCu_5F_3N_6O_{10}\cdot$ $CH_4O\cdot 2CH_2Cl_2$	$C_{82}H_{54}Cu_5F_3N_7O_{13}\cdot$ $1.91CH_4O\cdot 0.13H_2O$	$C_{82}H_{49}Cu_5F_9N_6O_{13}\cdot$ $3.7CH_2Cl_2$
M	195.2	1895.4	1783.4	2153.2
Crystal system	Monoclinic	Monoclinic	Triclinic	Triclinic
Space group	$P2_1/n$	$P2_1/n$	$P\bar{1}$	$P1$
a/Å	5.887(4)	19.317(14)	12.021(8)	13.299(4)
b/Å	16.047(4)	19.133(14)	16.822(8)	16.292(5)
c/Å	10.697(3)	24.03(2)	23.058(17)	22.808(7)
α/°	90	90	92.05(5)	86.74(3)
β/°	92.27(4)	108.82(6)	94.95(7)	89.85(2)
γ/°	90	90	110.59(4)	68.60(2)
$U/Å^3$	1010	8410	4338	4529
Z	4	4	2	2
$D_c/g\ cm^{-3}$	1.280	1.497	1.365	1.579
Crystal size/mm	0.54 × 0.27 × 0.16	0.51 × 0.31 × 0.04	0.35 × 0.23 × 0.19	0.31 × 0.27 × 0.12
Crystal shape and colour	Colourless slab	Green plate	Green block	Green tablet
Radiation	Cu-Kα	Cu-Kα	Mo-Kα	Cu-Kα
μ/mm^{-1}	0.62	3.43	1.28	4.02
Unique data	1314	9561	11 950	13 287
Observed data	1135	4876	7751	7431
Parameters	137	1046	1032	1126
Restraints	0	113	72	66
Max. Δ/σ ratio	0.007	−0.048	−0.019	0.028
$R1$, $wR2$[a] (wR for Hpehp)	0.0468, 0.0602	0.0744, 0.1995	0.0821, 0.2754	0.0966, 0.2586
Weighting scheme, w^{-1}[b]	Chebychev three-term polynomial	$[\sigma^2(F_o^2) + (0.0871P)^2]$	$[\sigma^2(F_o^2) + (0.1215P)^2 + 29.5P]$	$[\sigma^2(F_o^2) + (0.1599P)^2]$
Goodness of fit	0.821	1.006	1.055	0.953
Largest residuals/e $Å^{-3}$	+0.15, −0.16	+0.621, −0.576	+1.187, −0.857	+1.242, −1.776

[a] $R1$ based on observed data, $wR2$ on all unique data. Refinement on F for Hpehp and F^2 for **1**–**3**. [b] $P = \frac{1}{3}[\max(F_o^2, 0) + 2F_c^2]$.

these were refined with similarity restraints on the C−F distances and FCF angles, while the anisotropic displacement parameters of pairs of fluorine atoms either opposite one another or very close to one another were constrained to be equal. In addition to two molecules of ordered CH_2Cl_2 in the structure of **3** it was clear from Δ*F* maps that there were two more regions containing disordered CH_2Cl_2 molecules. These (amounting to 1.4 CH_2Cl_2 per formula unit) were treated in the manner described in reference 16. In **1** phenyl groups 1 and 3 are rotationally disordered about a common pivot atom [C(91) and C(93) respectively]. In ring 1 the geometry of the ring was restrained explicitly, with common isotropic thermal parameters for chemically equivalent atoms; ring 3 was restrained to have two-fold symmetry and independent isotropic thermal parameters refined for each atom. The CF_3 groups in **1** and **2** were rotationally disordered and treated as described above for **3**.

Table 2 Selected bond distances (Å) and angles (°) for Hpehp

N(1)−C(2)	1.367(3)	C(7)−C(8)	1.199(3)
N(1)−C(6)	1.378(2)	C(8)−C(9)	1.431(3)
C(2)−C(3)	1.362(3)	C(9)−C(10)	1.395(3)
C(2)−C(7)	1.427(3)	C(9)−C(14)	1.396(3)
C(3)−C(4)	1.412(3)	C(10)−C(11)	1.380(3)
C(4)−C(5)	1.350(3)	C(11)−C(12)	1.382(3)
C(5)−C(6)	1.427(3)	C(12)−C(13)	1.367(3)
C(6)−O(6)	1.252(2)	C(13)−C(14)	1.381(3)
C(2)−N(1)−C(6)	123.7(2)	C(2)−C(7)−C(8)	175.3(2)
N(1)−C(2)−C(3)	120.4(2)	C(7)−C(8)−C(9)	178.4(2)
N(1)−C(2)−C(7)	115.1(2)	C(8)−C(9)−C(10)	120.8(2)
C(3)−C(2)−C(7)	124.5(2)	C(8)−C(9)−C(14)	119.9(2)
C(2)−C(3)−C(4)	117.9(2)	C(10)−C(9)−C(14)	119.3(2)
C(3)−C(4)−C(5)	121.6(2)	C(9)−C(10)−C(11)	119.5(2)
C(4)−C(5)−C(6)	120.8(2)	C(10)−C(11)−C(12)	120.9(2)
N(1)−C(6)−C(5)	115.6(2)	C(11)−C(12)−C(13)	119.6(2)
N(1)−C(6)−O(6)	119.6(2)	C(12)−C(13)−C(14)	120.9(6)
C(5)−C(6)−O(6)	124.9(2)	C(9)−C(14)−C(13)	119.8(2)

Atomic coordinates, thermal parameters, and bond lengths and angles have been deposited at the Cambridge Crystallographic Data Centre (CCDC). See Instructions for Authors, *J. Chem. Soc., Dalton Trans.*, 1997, Issue 1. Any request to the CCDC for this material should quote the full literature citation and the reference number 186/492.

Magnetic measurements

Variable-temperature magnetic measurements on complexes **1**–**3** in the region 1.8–300 K were made using a SQUID magnetometer (Quantum Design) with samples sealed in capsules. In all cases diamagnetic corrections for the sample holders were applied to the data. Diamagnetic corrections for the samples were determined from Pascal's constants[17] and literature values.[18]

Results and Discussion

Synthesis and characterisation of 6-(phenylethynyl)-2-pyridone (Hpehp)

The ligand, 6-(phenylethynyl)-2-pyridone (Hpehp) was synthesised in a three-step procedure (see Scheme 1). Firstly, treatment of 2,6-dibromopyridine with benzyl alcohol and potassium hydroxide in toluene using 18-crown-6 as a phase-transfer catalyst[19] gave the pyridine benzyl ether, 2-bromo-6-benzyloxypyridine in quantitative yield. Secondly, coupling of 2-bromo-6-benzyloxypyridine with phenylacetylene to give 2-benzyloxy-6-phenylethynylpyridine was achieved in high yield (70%) upon treatment with a catalytic amount of bis(triphenylphosphine)palladium dichloride–copper(I) iodide in diethylamine.[20] Thirdly, the benzyl protecting group was removed by treatment with trifluoroacetic acid using the procedure outlined by Marsh and Goodman,[21] to give $Hpehp\cdot 0.5CF_3CO_2H$ (83%). Pure Hpehp could be obtained by recrystallisation from ethyl acetate.

A single crystal of Hpehp was the subject of an X-ray diffraction study at 220 K. Selected bond distances and angles are given in Table 2. Fig. 1 shows a view of four Hpehp molecules, two of which have self associated into dimers by hydrogen bonding through the NH hydrogens and the oxygen functionalities. The C(6)−O(6) bond length [1.252(2) Å] is consistent

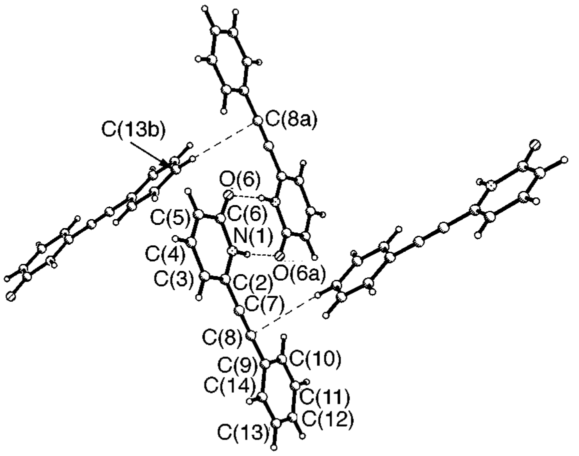

Fig. 1 Association of four molecules of Hpehp in the crystal, also showing the numbering scheme adopted

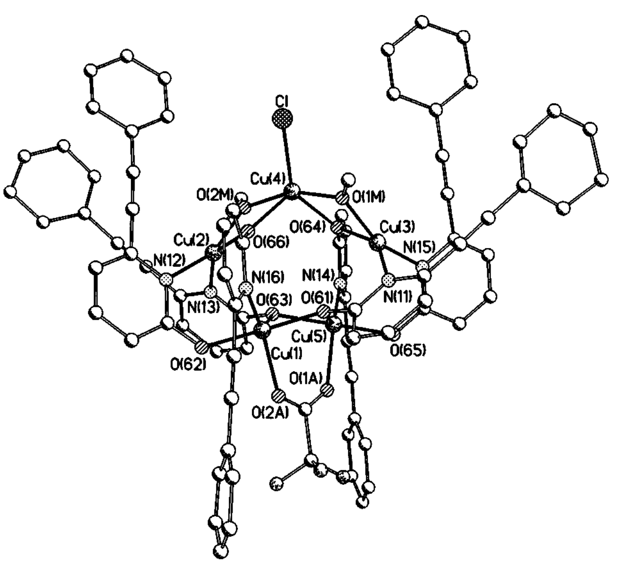

Fig. 2 Structure of **1** in the crystal showing the numbering scheme adopted

with a double bond supporting the preference for the 2-pyridone over the 2-pyridinol tautomer. A similar tautomeric preference is observed in the solid-state structure of 5-chloro-2-pyridone[22] while in the 6-halogeno-substituted derivatives, Hchp and Hbhp, the pyridinol tautomer is preferred.[23] Fig. 1 also shows possible but very weak C–H···C≡C hydrogen bonds between *p*-phenyl hydrogens of one molecule and the alkyne moiety of another [H(13b)···C(8a) 3.094(3), H(13b)···C(7a) 3.247(3) Å] which may be compared with the recently reported C–H···C≡C intermolecular contacts of 2.54 Å in DL-prop-2-ynylglycine.[24] The packing of molecules within the crystal of Hpehp also resembles that in DL-prop-2-ynylglycine with co-operative C–H···π interactions resulting in a zigzag arrangement of the dimeric 2-pyridone units.

The infrared data supports the preference for the pyridone over pyridinol tautomer with a well defined ν(NH) stretch occurring at 2932 cm^{-1}. In addition, IR reveals a ν(C≡C) band at 2213 cm^{-1} while the NH proton can be detected as a singlet at δ 12.35 in the room temperature ^{1}H NMR spectrum suggesting a strong hydrogen bond also exists in $CDCl_3$ solution.

Although pure Hpehp could be obtained from recrystallisation from ethyl acetate and was the subject of structural studies, reactions involving the trifluoroacetic acid adduct are reported below.

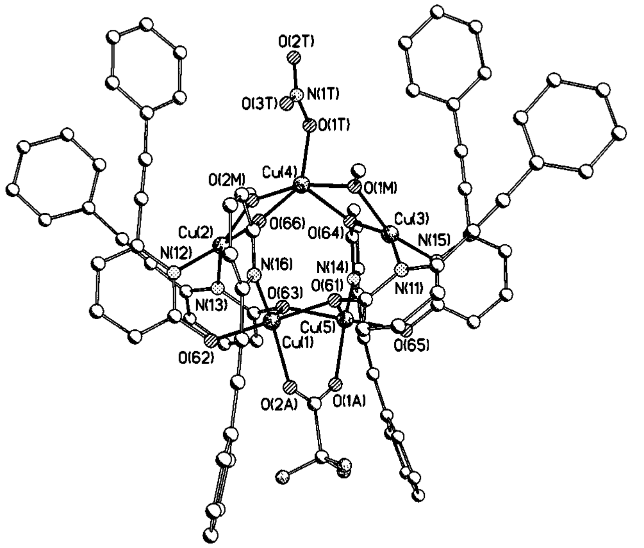

Fig. 3 Structure of **2** in the crystal showing the numbering scheme adopted

Synthesis and characterisation of complexes 1–3

The sodium salt of the Hpehp$\cdot$0.5CF_3CO_2H adduct was prepared by deprotonation with NaOH then mixed in a 2:1 ratio with hydrated copper(II) nitrate, and the two powders were ground together in a pestle and mortar. The resulting olive green paste was extracted with dichloromethane to give a dark green solution which was filtered to remove unreacted starting materials. The pentanuclear copper complexes **1**–**3** were crystallised as follows. The yields reported are for the crystalline material obtained. Selected bond distances and angles for all three structures are given in Tables 3 and 4.

(*i*) *Addition of methanol to the dichloromethane solution:* concentration of the dichloromethane solution and addition of an equal volume of methanol gave green plates in 55% yield after 2–3 d. A single crystal X-ray diffraction study at 220 K, showed a pentanuclear copper(II) complex of composition $[Cu_5(OMe)_2(CF_3CO_2)(pehp)_6(Cl)]$ **1**, a view of which is shown in Fig. 2.

(*ii*) *Addition of* $La(NO_3)_3\cdot 6H_2O$ *in methanol to the dichloromethane solution:* concentration of the dichloromethane solution and addition of an equal volume of methanol containing an excess of $La(NO_3)_3\cdot 6H_2O$ gave green blocks after 2–3 d (40%). A single crystal X-ray diffraction study at 220 K, revealed a closely related pentanuclear copper(II) complex with composition $[Cu_5(OMe)_2(CF_3CO_2)(pehp)_6(NO_3)]$ **2**, a view of which is shown in Fig. 3.

(*iii*) *Prolonged standing of a dichloromethane solution:* concentration of the dichloromethane solution and prolonged standing (*ca.* 3 w) at room temperature gave green plates in 10% yield. A single crystal X-ray diffraction study at 220 K revealed a less symmetric pentanuclear copper(II) complex of composition $[Cu_5(OH)(CF_3CO_2)_3(pehp)_6]$ **3**, which is shown in Fig. 4.

The structures of **1**–**3** (Figs. 2–4) are related with each containing five copper atoms held together by a variety of bridging ligands in a capped butterfly arrangement (Fig. 5). In **1** and **2** this array has pseudo-two-fold symmetry with a non-crystallographic axis passing through Cu(4) and the mid-point of the Cu(1)···Cu(5) vector. Complex **3** is less symmetric due to inequivalent cap–wingtip bridging ligands. The co-ordination numbers within the Cu_5 cores are the same with two four-co-ordinate copper atoms occupying the wingtip sites [Cu(2), Cu(3)] and three five-co-ordinate copper atoms occupying the body and cap sites [Cu(1), Cu(5), Cu(4)]. The four-co-ordinate sites have a distorted-square-planar geometry, while the five-co-ordinate sites can be described as distorted trigonal

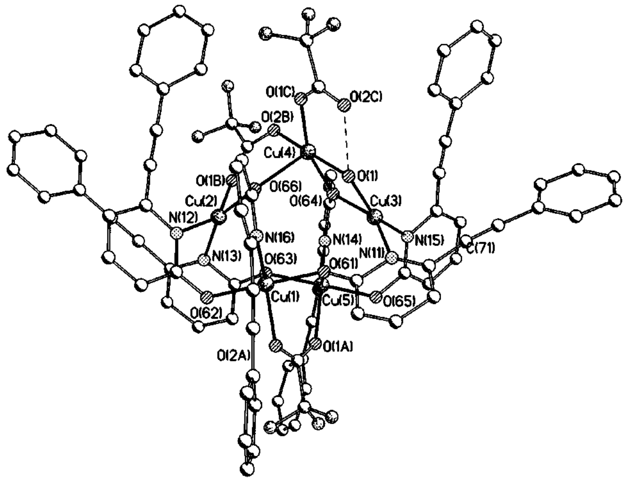

Fig. 4 Structure of **3** in the crystal showing the numbering scheme adopted

bipyramidal with the axial sites being defined at Cu(1), by O(61) and O(62) [O(61)–Cu(1)–O(62) *ca.* 167°] and at Cu(5), by O(63) and O(65) [O(63)–Cu(5)–O(65) *ca.* 169°] and at the capping Cu(4), by O(1M) and O(2M) in **1** and **2** [O(1M)–Cu(4)–O(2M): 159.2(3) **1**, 164.3(3)° **2**] while at Cu(4) for **3** by O(1) and O(2B) [O(1)–Cu(4)–O(2B): 170.4(3)°].

The co-ordination spheres of the copper centres in **1**–**3** are similar with each complex containing six deprotonated Hpehp molecules which bridge within the Cu_5 core through the exocyclic oxygen and ring nitrogen atoms in three different ways: (*i*) 1,3-bridging one site on the body and a wingtip [Cu(5) · · · Cu(3) and Cu(1) · · · Cu(2)]; (*ii*) 1,1′,3-bridging across the body and to a wingtip [Cu(1) · · · Cu(5) · · · Cu(3) and Cu(1) · · · Cu(5) · · · Cu(2)]; (*iii*) 1,1′,3-bridging the cap, a wingtip and one site on the body [Cu(4) · · · Cu(3) · · · Cu(1) and Cu(4) · · · Cu(3) · · · Cu(5)].

To complete the co-ordination spheres in **1**–**3** a further four monoanionic ligands are required. In **1** and **2** there are two bridging methoxide groups [wingtip–cap; Cu(2) · · · Cu(4), Cu(3) · · · Cu(4)], one body-bridging trifluoroacetate [Cu(1) · · · Cu(5)] and a terminally bound anion [Cl^- **1** or NO_3^- **2** on Cu(4)]. The source of the terminal chloride anion for **1** is presumably the CH_2Cl_2 solvent as the moderate, and reproducible, yield of **1** indicates this cannot be due to an impurity. In **3** there is one bridging hydroxide group [Cu(3)–O(H)–Cu(4)] and three trifluoroacetate groups, which are body bridging [Cu(1) · · · Cu(5)], one wingtip–cap bridging [Cu(2) · · · Cu(4)] and one terminal [Cu(4)].

The Cu · · · Cu distances within the complexes vary in a similar manner for both **1** and **2**. The shortest Cu · · · Cu contacts, 3.050(3) and 3.058(3) Å in **1** and 3.024(6) and 3.049(6) Å in **2**, occur between the capping Cu site [Cu(4)] and the wingtip Cu atoms [Cu(2) and Cu(3)]. One pair of body–wingtip contacts [Cu(1) · · · Cu(2) and Cu(3) · · · Cu(5)] are intermediate, 3.178(3) and 3.148(3) in **1** and 3.148(6) and 3.197(6) Å in **2**, and slightly shorter than the Cu(1) · · · Cu(5) contacts of 3.194(3) and 3.235(6) Å in **1** and **2** respectively. The second pair of body–wingtip contacts [Cu(1) · · · Cu(3) and Cu(2) · · · Cu(5)] are longer in both complexes; in **1** the contacts are 4.461(4) and 4.400(4) Å respectively, and in **2** 4.437(4) and 4.445(4) Å. This difference between the two pairs of body–wingtip contacts is a large distortion from an ideal tetrahedron, capped or otherwise.

Within such a distorted metal array the description chosen is somewhat arbitary, however alternative descriptions of the polyhedron, *e.g.* as a pentagon, are much less satisfactory than the description based on a capped butterfly. For a regular pentagon the Cu · · · Cu contacts should all be consistent, where here they vary from 3.050(3) to 3.194(3) Å in **1**, and from 3.024(4) to 3.235(6) Å in **2**. More seriously, four of the five internal angles of the 'pentagon' are in the range 88–92° for structures **1** and **2**, rather than close to 108° as required for a pentagon. Finally in both structures the 'pentagon' is far from planar, with the Cu(1) · · · Cu(5) vector at an angle of 36° to the mean plane of the other three Cu atoms within the cage.

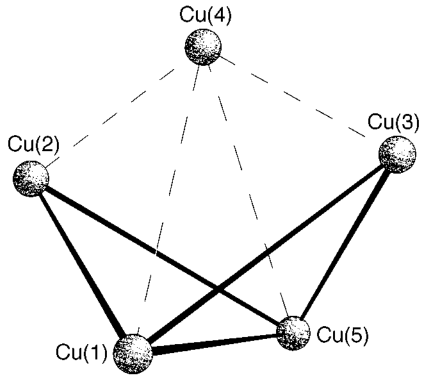

Fig. 5 'Capped-butterfly' metal polyhedron in **1**. The numbering of metal sites is common to **2** and **3**

In **3** the capping site [Cu(4)] is bridged to the two wingtip sites in dissimilar ways. The Cu(3) · · · Cu(4) vector is bridged by an hydroxide ligand and a μ-O from pehp, and this distance is similar [3.042(7) Å] to the equivalent contacts in **1** and **2**. The Cu(2) · · · Cu(4) vector is bridged by a trifluoroacetate group and a μ-O from pehp, and the contact of 3.638(7) Å is much longer. The remaining Cu · · · Cu distances in **3** are very similar to equivalent contacts in **1** and **2**. It is also noteworthy that the bridging hydroxide in **3** and the methoxide groups in **1** and **2** appear to exert the same structural requirements as exemplified both by the similar Cu(3) · · · Cu(4) distances and the Cu(4)–O(R)–Cu(3) angles [R = Me, 106.9(3) **1** *vs.* R = Me, 106.4(3) **2** *vs.* R = H, 107.7(3)° **3**].

Intramolecular hydrogen-bond interactions also play roles in the structures of **1**–**3** which seem to be of two types namely, C–H · · · O and C–H · · · C≡C. In **3** a conventional hydrogen-bond interaction exists between H(1) of the bridging hydroxide and O(2C) of the terminal trifluoroacetate on Cu(4) [H(1) · · · O(2C) 1.969(4) Å] while more unusually there exist some short C–H · · · C≡C contacts between pehp groups in all the structures. In **3** the *o*-phenyl hydrogen H(141) has a contact with an alkyne moiety [H(141) · · · C(85) 2.68; H(141) · · · C(75) 2.61 Å] which is significantly shorter than the C–H · · · C≡C intermolecular distance in Hpehp [H(13b) · · · C(8a) 3.09, H(13b) · · · C(7a) 3.25 Å] but compares well with the reported value of 2.54 Å in DL-prop-2-ynylglycine.[24] Therefore comparison of the structures of Hpehp and **3** suggests that the shortness of the contact in **3** is imposed by other structurally directing interactions, and is in itself unlikely to be of significance.

Complexes **1**–**3** were, in addition, characterised by infrared and mass spectrometry and by elemental analysis. It has previously been observed that the pyridonate-bridged species, $[Cu_6Na(mhp)_{12}][NO_3]$ and $[Cu_8(O)_2(O_2CR)_4(xhp)_8]$ (where R = CH_3, C_6H_5 or CF_3 and xhp = 6-chloro-, 6-bromo- or 6-methyl-pyridonate) give clear FAB-MS results so it was hoped similar good quality mass spectroscopic data would be observed for the pentanuclear complexes. Indeed, the FAB mass spectra for **1**–**3** gave sensible fragmentation peaks although the parent-ion peaks themselves were not seen. For example, in **2** peaks are seen for both $[Cu_5(OMe)(CF_3CO_2)(pehp)_6]$ (M^+ − OMe − NO_3) and $[Cu_5(CF_3CO_2)(pehp)_6]$ (M^+ − 2 OMe − NO_3), and a large number of polycopper fragments down to $[Cu_2(pehp)_2]$. A general observation for all the spectra is that the methoxide, trifluoroacetate and nitrate/chloride ligands tend to be lost first during the fragmentation to leave units of the general formula $[Cu_x(pehp)_y]$. The IR spectra of **1**–**3** were

Table 3 Selected bond distances (Å) for compounds **1**–**3**

Compound	**1**	**2**	**3**
Cu(1)···Cu(2)	3.178(3)	3.148(6)	3.156(7)
Cu(1)···Cu(5)	3.194(3)	3.235(6)	3.259(7)
Cu(2)···Cu(4)	3.058(3)	3.024(6)	3.638(7)
Cu(3)···Cu(4)	3.050(3)	3.049(6)	3.042(7)
Cu(3)···Cu(5)	3.148(3)	3.197(6)	3.206(7)
Cu(1)–O(61)	1.924(7)	1.937(6)	1.932(6)
Cu(1)–O(62)	1.908(7)	1.903(6)	1.922(6)
Cu(1)–O(63)	2.271(8)	2.351(7)	2.370(6)
Cu(1)–O(2A)	2.048(8)	2.020(7)	2.038(6)
Cu(1)–N(16)	2.000(9)	2.031(8)	1.999(7)
Cu(2)–N(12)	1.975(9)	1.984(8)	1.979(8)
Cu(2)–N(13)	1.971(9)	1.996(8)	1.979(7)
Cu(2)–O(66)	1.969(7)	1.970(6)	1.910(6)
Cu(2)–O(1B)			2.007(7)
Cu(2)–O(2M)	1.890(7)	1.895(7)	
Cu(3)–N(11)	1.976(9)	1.995(8)	1.976(8)
Cu(3)–N(15)	1.971(9)	1.958(8)	1.960(8)
Cu(3)–O(64)	1.971(7)	1.978(7)	2.000(6)
Cu(3)–O(1)			1.879(6)
Cu(3)–O(1M)	1.902(8)	1.900(7)	
Cu(4)–O(64)	2.131(7)	2.183(7)	2.010(6)
Cu(4)–O(66)	2.195(70	2.067(7)	2.249(6)
Cu(4)–O(1)			1.889(6)
Cu(4)–O(1M)	1.894(8)	1.907(7)	
Cu(4)–O(2B)			1.949(6)
Cu(4)–O(2M)	1.920(8)	1.929(6)	
Cu(4)–O(1C)			1.968(6)
Cu(4)–Cl	2.243(7)		
Cu(4)–O(1T)		2.087(11)	
Cu(5)–O(61)	2.263(7)	2.337(6)	2.418(6)
Cu(5)–O(63)	1.946(7)	1.944(6)	1.942(6)
Cu(5)–O(65)	1.911(8)	1.902(6)	1.875(7)
Cu(5)–O(1A)	2.072(8)	2.031(7)	2.015(6)
Cu(5)–N(14)	2.016(8)	2,017(8)	2.020(8)

Table 4 Selected bond angles (°) for compounds **1**–**3**

Compound	**1**	**2**	**3**
O(62)–Cu(1)–O(61)	166.7(3)	165.8(3)	168.9(3)
O(62)–Cu(1)–N(16)	94.9(3)	95.8(3)	93.0(3)
O(61)–Cu(1)–N(16)	94.8(3)	94.1(3)	94.9(3)
O(62)–Cu(1)–O(2A)	86.9(3)	86.8(3)	85.9(2)
O(61)–Cu(1)–O(2A)	92.2(3)	92.5(3)	91.1(2)
N(16)–Cu(1)–O(2A)	137.4(3)	138.6(3)	149.5(3)
O(62)–Cu(1)–O(63)	90.4(3)	89.9(3)	89.4(2)
O(61)–Cu(1)–O(63)	76.3(3)	75.9(2)	79.9(2)
N(16)–Cu(1)–O(63)	129.7(3)	128.3(3)	122.1(2)
O(2A)–Cu(1)–O(63)	92.8(3)	93.0(3)	88.4(2)
O(2M)–Cu(2)–O(66)	80.9(3)	79.0(3)	
O(2M)–Cu(2)–N(13)	98.7(4)	99.0(3)	
O(66)–Cu(2)–N(13)	147.3(4)	145.8(3)	154.5(3)
O(2M)–Cu(2)–N(12)	156.2(4)	156.6(3)	
O(66)–Cu(2)–N(12)	93.5(3)	95.9(3)	95.1(3)
O(66)–Cu(2)–O(1B)			93.6(3)
N(12)–Cu(2)–O(1B)			146.5(3)
N(13)–Cu(2)–O(1B)			91.6(3)
N(13)–Cu(2)–N(12)	98.4(4)	97.8(3)	94.1(3)
O(1M)–Cu(3)–O(64)	78.6(3)	79.4(3)	
O(1M)–Cu(3)–N(15)	157.7(4)	157.0(3)	
O(64)–Cu(3)–N(15)	96.2(3)	96.5(3)	93.5(3)
O(1M)–Cu(3)–N(11)	97.2(4)	98.2(3)	
O(64)–Cu(3)–N(11)	146.7(3)	147.9(3)	150.4(3)
N(15)–Cu(3)–N(11)	98.7(4)	97.0(3)	98.7(3)
O(1)–Cu(3)–N(15)			156.2(3)
O(1)–Cu(3)–N(11)			100.0(3)
O(1)–Cu(3)–O(64)			77.0(3)
O(1M)–Cu(4)–O(2M)	159.2(3)	164.3(3)	
O(1M)–Cu(4)–O(64)	74.9(3)	74.2(3)	
O(2M)–Cu(4)–O(64)	94.2(3)	96.6(3)	
O(1M)–Cu(4)–O(66)	93.8(3)	96.8(3)	
O(2M)–Cu(4)–O(66)	74.6(3)	75.8(3)	
O(64)–Cu(4)–O(66)	115.3(3)	117.3(3)	99.5(2)
O(1M)–Cu(4)–Cl	99.6(3)		
O(2M)–Cu(4)–Cl	100.9(3)		
O(64)–Cu(4)–Cl	129.9(2)		
O(66)–Cu(4)–Cl	114.7(2)		
O(1M)–Cu(4)–O(1T)		101.9(4)	
O(2M)–Cu(4)–O(1T)		91.7(3)	
O(66)–Cu(4)–O(1T)		144.5(4)	
O(1T)–Cu(4)–O(64)		96.8(4)	
O(1)–Cu(4)–O(2B)			170.4(3)
O(1)–Cu(4)–O(1C)			98.1(3)
O(2B)–Cu(4)–O(1C)			88.2(3)
O(1)–Cu(4)–O(64)			76.6(3)
O(2B)–Cu(4)–O(64)			95.0(3)
O(1C)–Cu(4)–O(64)			159.9(3)
O(1)–Cu(4)–O(66)			94.8(3)
O(2B)–Cu(4)–O(66)			91.1(2)
O(1C)–Cu(4)–O(66)			100.3(2)
O(65)–Cu(5)–O(63)	169.5(3)	166.2(3)	172.2(3)
O(65)–Cu(5)–N(14)	94.3(3)	96.1(3)	93.8(3)
O(63)–Cu(5)–N(14)	93.6(3)	93.5(3)	92.0(3)
O(65)–Cu(5)–O(1A)	85.3(3)	86.5(3)	84.6(3)
O(63)–Cu(5)–O(1A)	93.0(3)	92.3(3)	92.8(3)
N(14)–Cu(5)–O(1A)	140.4(3)	140.7(3)	152.4(3)
O(65)–Cu(5)–O(61)	93.5(3)	90.2(3)	94.1(3)
O(63)–Cu(5)–O(61)	76.1(3)	76.1(2)	78.4(2)
N(14)–Cu(5)–O(61)	130.0(3)	127.2(3)	121.1(2)
O(1A)–Cu(5)–O(61)	89.4(3)	91.9(3)	86.5(2)
Cu(4)–O(1M)–Cu(3)	106.9(3)	106.4(3)	
Cu(3)–O(1)–Cu(4)			107.7(3)
Cu(2)–O(2M)–Cu(4)	106.8(4)	104.5(3)	
Cu(1)–O(61)–Cu(5)	99.1(3)	98.0(3)	96.4(2)
Cu(5)–O(63)–Cu(1)	98.1(3)	97.3(3)	97.7(3)
Cu(3)–O(64)–Cu(4)	96.0(3)	94.1(3)	98.7(3)
Cu(2)–O(66)–Cu(4)	94.4(3)	97.0(3)	121.8(3)

also useful in identification with a number of clearly observable absorption bands. In addition to the alkyne stretch in the region 2113–2117 cm^{-1} seen for all the complexes, the intramolecular H-bond in **3** results in a ν(O–H) band at 3250 cm^{-1} while in **2** a $\nu(O_2N{-}O)$ band occurs at 1289 cm^{-1}.

While there are many structurally characterised pentanuclear Cu^{I} and mixed-valence Cu^{II}–Cu^{I} complexes in the literature[25] there are fewer examples of discrete pentameric Cu^{II} species.[26] Apart from $[Cu_5(bta)_6(acac)_4]$ (Hacac = pentane-2,4-dione, Hbta = benzotriazole)[26b] the structural motifs of the remaining Cu^{II}_5 are based on a square-planar tetrameric unit with the fifth Cu^{II} ion sitting in or above the plane. In $[Cu_5(bta)_6(acac)_4]$ a distorted-tetrahedral arrangement of four copper atoms has its fifth copper centre sitting in the centre of the tetrahedron. Therefore complexes **1**–**3** have a quite different metal polyhedron to any reported previously for Cu^{II}.

Magnetic studies of complexes 1–3

The magnetic properties of complexes **1**–**3** were studied over the temperature range 1.8–300 K in an applied field of 1000 G (0.1 T) (Fig. 6). All three complexes behave in an essentially identical manner. At room temperature the value for the product $\chi_m T$ (where χ_m is the molar magnetic susceptibility) is between 1.6 and 2.0 cm^3 K mol^{-1}, depending on sample. This value is consistent with, if slightly below, that calculated for five non-interacting copper(II) centres (for $g = 2.1$ a calculated value of $\chi_m T = 2.1$ cm^3 K mol^{-1}). As the temperature is lowered the value falls steadily, and for each sample reaches a low temper-

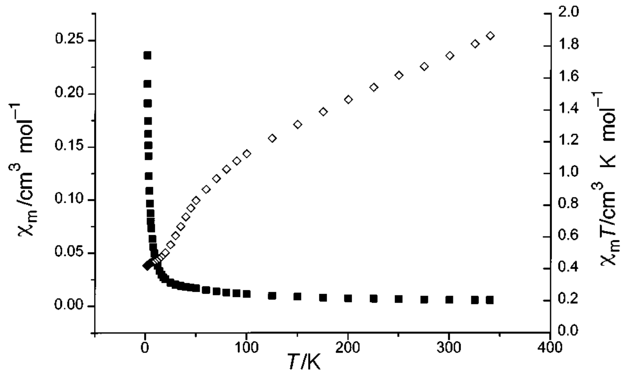

Fig. 6 Plots of χ_m and $\chi_m T$ against T for **1**. Similar behaviour is observed for **2** and **3**. χ_m is shown as full squares; $\chi_m T$ is shown as open diamonds

ature value consistent with an $S = \frac{1}{2}$ ground state. The exchange coupling is therefore predominantly antiferromagnetic, and comparatively weak as the room temperature value for $\chi_m T$ indicates occupation of all possible spin levels. The low symmetry of the structures would require at least three exchange integrals to model the data properly. As such a model would inevitably involve correlation of the values for the various exchange terms we do not feel it is worth pursuing, especially as the spin of the ground state is low.

The $S = \frac{1}{2}$ ground state was confirmed by EPR measurements at 3.6–10 K and Q-band. These show for each sample a broad resonance near $g = 2.15$. For **2** this signal could be interpreted as due to an axial system with g values of 2.22 and 2.08. Warming the sample to 80 K rendered this signal broader and isotropic. For **3** EPR studies also indicated presence of an uncoupled monomeric impurity which gave a typical spectrum for an isolated Cu^{II} centre.

Conclusion

By introduction of the phenylethynyl group to the sixth position of the pyridonate ring the reactivity towards copper salts has been varied. While octanuclear species are generated on reaction of copper(II) nitrate with xhp (x = Br, Cl or Me) and carboxylates, the corresponding reaction with pehp results in exclusively pentanuclear complexes. This structural variation is probably due to the bulky phenylethynyl substituent in the 6-position of the pyridone.

The formation of compound **1** by abstraction of chloride from CH_2Cl_2 was unexpected, and this reaction can be prevented by addition of a source of nitrate anions, to give **2**. What is interesting is that the pentanuclear core is preserved, suggesting that the metal cage is formed in solution prior to crystallisation, and that substitution reactions might be possible at the terminal co-ordination site on Cu(4).

Acknowledgements

We thank the EPSRC for funding for a diffractometer, and the Leverhulme Trust for funding a post-doctoral fellowship (A. A. D.). We also thank the Royal Society of Edinburgh for support (G. A. S.), and Drs. F. E. Mabbs and E. J. L. McInnes of the EPSRC c.w.e.p.r. centre at the University of Manchester for the Q-band spectra of **1**–**3**.

References

1 S. J. Lippard, *Angew. Chem., Int. Ed. Engl.*, 1988, **27**, 344.
2 A. Caneschi, A. Cornia, A. C. Fabretti and D. Gatteschi, *Angew. Chem., Int. Ed. Engl.*, 1995, **34**, 2862 and refs. therein.
3 A. K. Powell, S. L. Heath, D. Gatteschi, L. Pardi, R. Sessoli, R. Spina, F. Del Giallo and F. Pieralli, *J. Am. Chem. Soc.*, 1995, **117**, 2491.
4 E. Rentschler, D. Gatteschi, A. Cornia, A. C. Fabretti, A.-L. Barra, O. I. Shchegolikhina and A. A. Zhdanov, *Inorg. Chem.*, 1996, **35**, 4427 and refs. therein.
5 J. M. Rawson and R. E. P. Winpenny, *Coord. Chem. Rev.*, 1995, **139**, 313.
6 A. J. Blake, C. M. Grant, E. J. L. McInnes, F. E. Mabbs, P. E. Y. Milne, S. Parsons, J. M. Rawson and R. E. P. Winpenny, *J. Chem. Soc., Dalton Trans.*, 1996, 4077.
7 A. J. Blake, C. M. Grant, S. Parsons and R. E. P. Winpenny, *J. Chem. Soc., Dalton Trans.*, 1995, 1765.
8 A. J. Blake, R. O. Gould, P. E. Y. Milne and R. E. P. Winpenny, *J. Chem. Soc., Chem. Commun.*, 1991, 1453.
9 A. J. Blake, C. M. Grant, S. Parsons, J. M. Rawson, D. Reed and R. E. P. Winpenny, *J. Chem. Soc., Dalton Trans.*, 1995, 163.
10 Y. Ducharme and J. D. Wuest, *J. Org. Chem.*, 1988, **53**, 5788.
11 J. Cosier and A. M. Glazier, *J. Appl. Crystallogr.*, 1986, **19**, 105.
12 A. Altomare, M. C. Burla, M. Camelli, G. Cascarano, C. Giacovazzo, A. Guagliardi and G. Polidori, *J. Appl. Crystallogr.*, 1994, **27**, 435.
13 G. M. Sheldrick, SHELXS 86, program for crystal structure solution, *Acta Crystallogr., Sect. A*, 1990, **46**, 467.
14 D. J. Watkin, J. R. Curruthers, C. K. Prout and P. W. Betteridge, CRYSTALS, ISSUE 10, Chemical Crystallography Laboratory, University of Oxford, 1996.
15 G. M. Sheldrick, SHELXL 93, program for crystal structure refinement,University of Göttingen, 1993.
16 P. van der Sluis and A. L. Spek, *Acta Crystallogr., Sect. A.*, 1990, **46**, 194.
17 C. J. O'Connor, *Prog. Inorg. Chem.*, 1982, **29**, 203.
18 *Handbook of Chemistry and Physics*, ed. R. C. Weast, CRC Press, Boca Raton, FL, 70th edn., 1990, p. E134.
19 A. J. Serio Duggan, E. J. J. Grabowski and W. K. Russ, *Synthesis*, 1980, 573.
20 K. Sonogasira, Y. Tohda and N. Hagihara, *Tetrahedron Lett.*, 1975, 4467.
21 J. P. Marsh and L. Goodman, *J. Org. Chem.*, 1965, **30**, 2491.
22 A. Kvick, *Acta Crystallogr., Sect. B*, 1976, **32**, 220.
23 A. Kvick and I. Olovsson, *Ark. Khim.*, 1968, **30**, 71; A. Kvick and S. S. Booles, *Acta Crystallogr., Sect. B*, 1972, **28**, 3405.
24 T. Steiner, *J. Chem. Soc., Chem. Commun.*, 1995, 95.
25 See for example, L. P. Wu, M. Yamamoto, T. Kuroda-Sowa, M. Maekawa, Y. Suenaga and M. Munakata, *J. Chem. Soc., Dalton Trans.*, 1996, 2031; G. M. Kapteijn, I. C. M. Wehman-Ooyevaar, D. M. Grove, W. J. J. Smeets, A. L. Spek and G. van Koten, *Angew. Chem.*, 1993, **32**, 72; A. Eichhöfer, D. Fenske and W. Holstein, *Angew. Chem.*, 1993, **32**, 242.
26 (*a*) B. R. Gibney, D. P. Kesissoglou, J. W. Kampf and V. L. Pecoraro, *Inorg. Chem.*, 1994, **33**, 4840; (*b*) J. Handley, D. Collison, C. D. Garner, M. Helliwell, R. Docherty, J. R. Lawson and P. A. Tasker, *Angew. Chem.*, 1993, **32**, 1036; (*c*) S. Meenakumari and A. R. Chakravarty, *J. Chem. Soc., Dalton Trans.*, 1992, 2305; (*d*) B. Kurzak, E. Farkas, T. Glowiak and H. Kozlowski, *J. Chem. Soc., Dalton Trans.*, 1991, 163; (*e*) E. Gojon, J. Gaillard, J.-M. Latour and J. Laugier, *Inorg. Chem.*, 1987, **26**, 2046.

Received 6*th January* 1997; *Paper* 7/00107J